© Strojniški vestnik 47(2001)8,537-549
ISSN 0039-2480
UDK 536.2
Izvirni znanstveni članek (1.01)

© Journal of Mechanical Engineering 47(2001)8,537-549
ISSN 0039-2480
UDC 536.2
Original scientific paper (1.01)

THERMAL CONVECTION OF VISCOELASTIC FLUID WITH BIOT BOUNDARY CONDUCTION

Demir Huseyin
Department of Mathematics
Arts and Science Faculty
Ondokuz Mayis University
55139 Kurupelit-Samsun,
TURKEY

ABSTRACT:

Two-dimensional unsteady natural convection of a non-linear fluid represented by Criminale-Erickson-Filbey (CEF) fluid model in a square cavity is studied in the fluid for Rayleigh Benard convection case. The governing vorticity and energy transport equations are solved numerically either simple explicit and A.D.I. methods respectively. The two-dimensional convective motion is generated by bouyancy forces on the fluid fluid in a square cavity, when the vertical walls are either perfectly insulated or conducted with Biot boundary conduction condition. The contributions of the elastic and shear dependent characteristics of the liquid to the non-Newtonian behaviour are investigated on the temperature distribution and heat transfer. The effect of the Weissenberg (which is a measure of the elasticity of the fluid), Rayleigh and Biot numbers on the temperature and streamline profiles are delineated and this has been documented first time for the viscoelastic fluid.

INTRODUCTION

Two dimensional natural convection heat transfer of a non-linear fluid in enclosures of rectangular cross section is encountered in many practical situations due to its wide application in various engineering devices, which involve heat transfer across double glazing windows, solar energy, the electrical and nuclear industries, sterilisation of foods, building insulation. Such flows are also of interest in geophysics and can be applied in the circulation of the atmosphere and of magma in the Earth's upper mantle. Many fluids exhibit non-Newtonian behaviour in industrial applications, but there are very few studies reported for natural convection based on non-Newtonian fluids in the literature for both viscoinelastic or viscoelastic fluids. Therefore concerning the natural convection of visco-elastic fluids are almost non-existent. Review of the literature for two dimensional free convection in rectangular enclosures can be found in references (Shoney, 1988), (Gebhard et.al., 1988), (Demir, 1996) and (Demir et.al., 2000).

In this work, we examine two dimensional Rayleigh-Benard convection for visco-elastic fluid namely CEF fluid in a horizontal enclosure of cross section heated from below is studied when two vertical sides are insulated or conducted with Biot boundary condition with shear-free boundary conditions. Rayleigh-Benard convection one of the best known problem of fluid mechanics and has been subject of theoretical research and this problem has been investigated by many researchers with various aims due to its practical applicability.

In this paper we present numerical results for Rayleigh-Benard convection conducted with Biot boundary condition in a horizontal cavity with heating from below. In general, the use of this type of model would give realistic results in motions with small strain rates. In free convection ,although the strains may be large, the strain rates are relatively small. In most buoyancy driven motions is also slow due to moderate temperature gradient. Therefore, CEF model is ideally suited for the study of this class motions. This provide the motivation for the present work where the effect of the Weissenberg number on the flow field explored numerically first time. For calibration of the code,

firstly two dimensional plane natural convection of the Newtonian fluid in a square cavity is solved. Excellent agreement is found with the work of (De Vahl 1983), (Torrance&Turcotte, 1971) and (Mckenzie, 1974). Then for further calibration of the code, two dimensional plane natural of a viscous pseudoplastic flow in a square cavity is studied. The recirculating flow are depicted properly in detail along with the temperature distributions which has not been given before in detail. Following this, to test the capabilities of the code Weissenberg effect on the flow field for CEF fluid is studied. Finally, the dependence of the Nusselt number on the characteristics is investigated.

MATHEMATICAL FORMULATION

We consider the flow regime in a two dimensional square cavity as discussed reference (Demir, 1996). The two end walls are kept at different temperatures $T_1 > T_0$ and the remaining walls are insulated or conducted with Biot boundary conditions. The square enclosure considered is assumed to be very long in the third dimension. Then the governing differential equations subject to Boussinesq approximation are

$$\rho C_v \frac{DT}{Dt} = k\nabla^2 T + \Phi, \quad \nabla.\mathbf{u}=0 \qquad (2.1)$$

$$\left.\begin{aligned} \rho\frac{D\mathbf{u}}{Dt} &= -\nabla.\phi + \rho g\alpha\ \mathbf{e_y}(T-T_0) \\ &+ \nabla.\mathbf{S}^* \end{aligned}\right\} \qquad (2.2)$$

where $\mathbf{S}^*$ is the extra stress and ϕ is the reduced pressure field, $\phi = p - p_0$, p_0 = static pressure . ρ, α and k are the density, and the coefficient of thermal expansivity and thermal conductivity respectively, all evaluated at some average temperature. The operators D/Dt is the material time derivative $\partial/\partial t + \mathbf{u}.\nabla$.

For the CEF model, the extra stress can be written as

$$\left.\begin{aligned} S^*_{ik} &= 2\eta_s(\dot\gamma)d_{ik} + 4\chi(\dot\gamma)d_{ij}d_{jk} \\ &- 2\zeta(\dot\gamma)\overset{\nabla}{d}_{ik} \end{aligned}\right\} \qquad (2.3)$$

where d_{ik} is the first rate of strain tensor given by

$$d_{ik} = \frac{1}{2}\left(\frac{\partial u_i}{\partial x_k} + \frac{\partial u_k}{\partial x_i}\right). \qquad (2.4)$$

$\eta_s\left(\dot\gamma\right)$ is known as solvent viscosity and is a function of the second rate-of-strain invariant $\dot\gamma^2 = 2d_{ik}d_{ik}$. For our case we find that

$$\dot\gamma^2 = 4\left(\frac{\partial u}{\partial x}\right)^2 + \left(\frac{\partial u}{\partial y} + \frac{\partial v}{\partial x}\right)^2. \qquad (2.5)$$

In general the viscosity function $\eta_s\left(\dot\gamma\right)$ should be continuous, well defined and able to attain a finite zero shear-rate viscosity. Consequently the viscosities are calculated using the Cross model

$$\frac{\eta - \eta_\infty}{\eta_0 - \eta_\infty} = \frac{1}{1+\left(\lambda\dot\gamma\right)^{(1-n)}}, \qquad (2.6)$$

where η_0 and η_∞ refer to the asymptotic values of viscosity at very low and very high shear rates respectively λ is a constant parameter with the dimension of time n is a dimensionless constant.

Here, $\chi\left(\dot\gamma\right)$ and $\varsigma\left(\dot\gamma\right)$ generally are defined as

$$4\chi\left(\dot\gamma\right) = N_2\left(\dot\gamma\right),\ 2\varsigma\left(\dot\gamma\right) = N_1\left(\dot\gamma\right), \qquad (2.7)$$

where $N_1\left(\dot\gamma\right)$ and $N_2\left(\dot\gamma\right)$ are material functions known as the primary and secondary normal stress coefficients, respectively. However, in this work, we use the following forms of this

$$\text{(i) } N_1 = 2\lambda_1\frac{\left(\eta_0 - \eta_\infty\right)}{1+\left(\lambda\dot\gamma\right)^{1-n}} \qquad (2.8)$$

(ii) $N_2 = 0$,

and upper convected derivatives in equation(2.3) is defined as

$$\overset{\nabla}{d}_{ik} = \frac{D}{Dt}d_{ik} - Ld_{ik} - d_{ik}L^T, \qquad (2.9)$$

where

$$L = \nabla V_i \ \text{ and } \ L^T = \left(\nabla V_i\right)^T. \qquad (2.10)$$

Now, substituting $S^*_{ik} = 2\eta_s(\dot\gamma)d_{ik} + \sigma^*_{ik}$ in Eqs.(2.2)-(2.3), the stress constitutive equation and stress equation of motion in the form of Elastic- Viscous pseudoplastic-Split-Stress (EV^{p}SS) which is similar to the Elastic Viscous Split Stress(EVSS) form of (Rajagopalan et al., 1990) can be written as

$$S^*_{ik} = 2\eta_s(\dot\gamma)d_{ik} + \sigma^*_{ik}, \qquad (2.11)$$

where

$$\sigma_{ik}^{\bullet} = -N_1(\dot{\gamma})\overset{\nabla}{d}_{ik}, \tag{2.12}$$

$$\left.\begin{aligned}\rho\left[\frac{\partial u}{\partial t}+u\frac{\partial u}{\partial x}+v\frac{\partial u}{\partial y}\right] &= -\frac{\partial \phi}{\partial x}+\frac{\partial}{\partial x}\left[2\eta_s\left(\dot{\gamma}\right)\frac{\partial u}{\partial x}\right]\\ &+\frac{\partial}{\partial y}\left[\eta_s\left(\dot{\gamma}\right)\left(\frac{\partial u}{\partial y}+\frac{\partial v}{\partial x}\right)\right]\\ &+\frac{\partial}{\partial x}\sigma_{xx}^{\bullet}+\frac{\partial}{\partial y}\sigma_{xy}^{\bullet}\end{aligned}\right\} \tag{2.13}$$

$$\left.\begin{aligned}\rho\left[\frac{\partial v}{\partial t}+u\frac{\partial v}{\partial x}+v\frac{\partial v}{\partial y}\right] &= -\frac{\partial \phi}{\partial y}\\ &+\rho g\alpha\left(T-T_0\right)\frac{\partial}{\partial x}\left[\eta_s\left(\dot{\gamma}\right)\left(\frac{\partial u}{\partial y}+\frac{\partial v}{\partial x}\right)\right]\\ &+\frac{\partial}{\partial y}\left[2\eta_s\left(\dot{\gamma}\right)\frac{\partial v}{\partial y}\right]+\frac{\partial}{\partial x}\sigma_{xy}^{\bullet}+\frac{\partial}{\partial y}\sigma_{yy}^{\bullet}\end{aligned}\right\} \tag{2.14}$$

For a 2-D planar case, if the velocities are defined as

$$u=\frac{\partial \psi^{\bullet}}{\partial y}, v=-\frac{\partial \psi^{\bullet}}{\partial x},\quad \omega=\frac{\partial v}{\partial x}-\frac{\partial u}{\partial y}, \tag{2.15}$$

and non-dimensional variables are introduces as

$$\left.\begin{aligned}X=\frac{x}{L}, Y=\frac{y}{L}, \tau=\frac{t\eta_0}{\rho L}\\ U=\frac{u\eta_0}{\rho L}, V=\frac{v\eta_0}{\rho\ L}, \overline{\eta}=\frac{\eta}{\eta_0}\end{aligned}\right\} \tag{2.16}$$

$$\Psi=\frac{\Psi^{\bullet}\eta_0}{\rho}, \theta=\frac{(T-T_0)}{(T_1-T_0)}, \Omega=\frac{\omega\eta_0}{\rho L^2}. \tag{2.17}$$

Then, taking the curl of the equation of motion which eliminates the unknown reduce pressure gradient, the resulting differences of the local velocity gradients can be abbreviated by the vorticity function ω. Thus ,the partial differential equation for stream function, vorticity, stresses and energy equation can be written as

$$\Omega=-\nabla^2\Psi, \tag{2.18}$$

$$\left.\begin{aligned}\frac{\partial\Omega}{\partial\tau} &= \frac{1}{\eta\,\mathrm{Re}}H\left(\overline{\eta}^{-2};\Omega\right)\\ &-\overline{\eta}\left\{U\frac{\partial\Omega}{\partial X}+V\frac{\partial\Omega}{\partial Y}\right\}+Gr\frac{\partial\theta}{\partial Y}+\frac{1}{\mathrm{Re}}F\end{aligned}\right\} \tag{2.19}$$

where

$$H\left(\overline{\eta}^{-2};\Omega\right)=\left\{\begin{aligned}&\frac{\partial}{\partial X}\left(\overline{\eta}^{-2}\frac{\partial\Omega}{\partial X}\right)\\ &+\frac{\partial}{\partial Y}\left(\overline{\eta}^{-2}\frac{\partial\Omega}{\partial Y}\right)\end{aligned}\right\} \tag{2.20}$$

$$\left.\begin{aligned}F &= M(\Omega)M\left(\overline{\eta}\right)+L(\Omega)L\left(\overline{\eta}\right)\\ &-\frac{1}{2}M\left(\sigma_{xx}-\sigma_{yy}\right)-L\left(\sigma_{xy}\right)\end{aligned}\right\} \tag{2.21}$$

and the operators is defined as

$$\left.\begin{aligned}M(\bullet) &= 2\frac{\partial^2}{\partial X\partial Y}\\ L(\bullet) &= \left(\frac{\partial^2(\bullet)}{\partial Y^2}-\frac{\partial^2(\bullet)}{\partial X^2}\right)\end{aligned}\right\} \tag{2.22}$$

$$\left.\begin{aligned}\frac{\partial\theta}{\partial\tau} &= \frac{1}{\mathrm{Pr}\,\mathrm{Re}}\nabla^2\theta\\ &-\left\{\frac{\partial}{\partial X}(U\theta)+\frac{\partial}{\partial Y}(V\theta)\right\}+\frac{Ec}{\mathrm{Re}}\Phi\end{aligned}\right\} \tag{2.23}$$

$$\left.\begin{aligned}\sigma_{xx} &= -2WeN\left[\begin{aligned}&\frac{\partial}{\partial\tau}\frac{\partial U}{\partial X}+U\frac{\partial^2 U}{\partial X^2}+V\frac{\partial^2 U}{\partial X\partial Y}\\ &-2\left(\frac{\partial U}{\partial X}\right)^2-\left(\frac{\partial U}{\partial Y}\right)^2-\left(\frac{\partial V}{\partial X}\frac{\partial U}{\partial Y}\right)\end{aligned}\right]\\ \sigma_{xy} &= -2WeN\left[\begin{aligned}&\frac{\partial}{\partial\tau}\frac{1}{2}\left(\frac{\partial U}{\partial Y}+\frac{\partial V}{\partial X}\right)\\ &+\frac{U}{2}\left(\frac{\partial^2 U}{\partial X\partial Y}+\frac{\partial^2 V}{\partial X^2}\right)\\ &+\frac{V}{2}\left(\frac{\partial^2 U}{\partial Y^2}+\frac{\partial^2 V}{\partial X\partial Y}\right)\\ &-\left(\frac{\partial V}{\partial Y}\frac{\partial U}{\partial Y}\right)-\left(\frac{\partial V}{\partial X}\frac{\partial U}{\partial X}\right)\end{aligned}\right]\\ \sigma_{xx} &= -2WeN\left[\begin{aligned}&\frac{\partial}{\partial\tau}\frac{\partial V}{\partial Y}+U\frac{\partial^2 V}{\partial X\partial Y}++V\frac{\partial^2 V}{\partial Y^2}\\ &-2\left(\frac{\partial V}{\partial Y}\right)^2-\left(\frac{\partial U}{\partial X}\right)^2-\left(\frac{\partial V}{\partial X}\frac{\partial U}{\partial Y}\right)\end{aligned}\right]\end{aligned}\right\} \tag{2.24}$$

On taking the non-dimensionalised form of the governing equations we have several non-dimensional parameters namely the Grashof number(Gr), the Prandtl number(Pr), the Eckert number (Ec).and Weissenberg number(We). The Grashof number is a measure of the ratio of buoyancy force to viscous effects within the flow and defined as $Gr=\left.g\rho^2\beta L^3\left(T_1-T_0\right)\right/\eta_0^2$ while the

Prandtl number is a measure the ratio of the fluid's kinematic viscosity to the thermal conductivity constant k and defined as $\Pr = {C_v \eta}/{k}$. The Eckert number is a measure of the viscous heating or the viscous dissipation part of the energy equation and defined as $Ec = {U^2}/{C_v(T_1 - T_0)}$. The product of Pr and Gr gives the Rayleigh number Ra. The We number is the measure of the elasticity of the fluid and is defined as ${\lambda_1 u}/{L}$ and N is a dimensionless form of ${2(\eta_0 - \eta_\infty)}/{\left(1+(\lambda\dot{\gamma}\right)^{1-n}}$.

The dimensionalles boundary and initial conditions that correspond to our problem are

$\tau \le 0$ whole space $\theta = \Omega = \Psi = U = V = 0$

$\tau > 0 \quad U = V = \Psi = \Omega = 0,$

$$\sigma_{xx} = \frac{-2We\dfrac{\partial^2 U}{\partial Y^2}}{1+\left(\lambda\left|\dfrac{\partial U}{\partial Y}\right|\right)^{1-n}},$$

$$\sigma_{xy} = \frac{We\dfrac{\partial^2 U}{\partial \tau \partial Y}}{1+\left(\lambda\left|\dfrac{\partial U}{\partial Y}\right|\right)^{1-n}}$$

$,\sigma_{xy} = 0$

at $X = 0$ and $X = 1$.

$\tau > 0 \quad U = V = \Psi = \Omega = 0,$

$\sigma_{xx} = 0,$

$$\sigma_{xy} = \frac{-We\dfrac{\partial^2 V}{\partial \tau \partial Y}}{1+\left(\lambda\left|\dfrac{\partial V}{\partial X}\right|\right)^{1-n}},$$

$$\sigma_{yy} = \frac{2We\dfrac{\partial^2 V}{\partial X^2}}{1+\left(\lambda\left|\dfrac{\partial V}{\partial X}\right|\right)^{1-n}}$$

at $Y = 0$ and $Y = 1$.

Also we have $\theta = 0$ at $Y = 1$, $\theta = 1$ at $Y = 0$ and $\dfrac{\partial \theta}{\partial X} = Bi(T - T_0)$ at $X = 1$ and $\dfrac{\partial \theta}{\partial X} = -Bi(T - T_0)$ at $X = 0$. Here T_0 used as the temperature of the cold wall and Bi used as Biot number. The local Nusselt numbers can be calculated from the temperature distribution as follows:

$$Nu = \left|\frac{\partial \theta}{\partial Y}\right|_{wall} \qquad (2.25)$$

METHOD OF SOLUTION AND GRID INDEPENDENCE

The modified equations were solved on a square mesh by a finite difference method; second -order central differences were used for all space variables and a fully implicit scheme for evaluating the time derivatives as described (Doughlas et.al., 1966) In the present work, the mixed eqs (2.1)-(2.2) are solved by the Alternating Direction Implicit (ADI) method developed by Peacemann-Rachford (Scraton, 1987) and (Mortom et.al., 1994) and tridiagonal matrix algorithm for solving the discretized equations. The elliptic stream function is solved iteratively using the Successive-Over-Relaxation (SOR) procedure. ADI method was used for this investigations because of earlier experience with this method in problems of buoyancy induced flow and heat transfer(e.g. De Vahl Davis, 1983).Richardson's extrapolation has been used ; this leads to the high accuracy bench mark solution as described in (Rajagopalan et al., 1990). Grid and time independence are carefully tasted as shown in Fig. 1. We also tested our computer code against the earlier published numerical result of (De Vahl, 1983), (Torrance et.al., 1971) and (Mc Kensie et.al., 1974) for accuracy and excellent agreement was found.

RESULTS AND DISCUSSION

In order to compare our original results, we present the streamline structure and temperature distribution for viscous pseudoplastic and CEF fluid together for the problem under consideration. In the results presented, Rayleigh ,Eccert and Weissenberg numbers are set at $10^4 \le Ra \le 10^6$, 0 and $0 \le We \le 0.01$,respectively. Despite, the evident progress over the last few years, obtaining accurate numerical solutions(or worse, any solution at all) at high values of the Weissenberg number(We) remains a challenge. The high Weissenberg number problem, i.e. the divergence of conventional iterative schemes beyond some critical value of the Weissenberg number, has been reported in virtually all published works (Charles et.al., 1989). There are several reason for this as discussed in(Charles et.al.,

1989). Despite, our work limited to the small values of the Weissenberg number, we found interesting structural changes in both streamline and temperature profiles as Weissenberg number increased from zero and as Biot number increased from zero.

For a viscous fluid, it was found one cell filled whole cavity at $Ra = 10^4$ which can be seen in Fig. 1 and it is symmetric both horizontally and vertically for Bi=0, but while the Bi number increases the flow produce to two mirror image counter rotating rectangular cells for viscous fluid as shown in Fig. 3. The corresponding temperature profiles are shown in Figs. 2-4 respectively. In Fig. 2 warm fluid rises near the bottom wall and cold fluid descends along the top and in Fig. 4, the colder fluid descends near the cavity's centre while the warm fluid rises nn convective motion near the walls. As Weissenberg number increases, in this case, the CEF fluid flow results show that the fluid exhibit similar behaviour when We number is used with or without the Bi number, we have one vortex with the direction of rotation as shown in Figs. 5-7. The corresponding temperature profiles are shown in Figs. 6-8 respectively, where warm fluid rises near the bottom and left walls and cold fluid descends along the top and right walls. The last one of them indicates that the left of cavity always warmer than right and warm fluid rises near the left wall. We are unable to get stable solution for $We \geq 0.01$, therefore we indicate the this value of the We number as $We_{crit.}$ and it is appeared to be impossible (as far as we know) to have stable solution beyond that value. This conclusion also indicate that the critical Weissenberg number is not artefact of our method.

We have one cell vortex at $Ra = 10^5$ in Fig. 9 for viscous fluid and it is show that the steady solution gives one large vortex which fills almost the whole cavity for Bi=0, but while the Bi number increases the flow produce to two mirror image counter rotating rectangular cells for viscous fluid as shown in Fig. 11. The corresponding temperature profiles are given in Figs 10-12. In Fig(10) the temperature throughout most of the cavity is uniform obtaining a value which average of the top and bottom walls. The second Fig. 12 indicates that. the colder fluid descends near the cavity's centre while the warm fluid rises in convective motion near the walls. As Weissenberg number increases, in this case, the CEF fluid flow results show that the flow emerged as two unequal cells and they were not symmetric and one vortex dominant to other vortex for viscous fluid as shown in Fig. 13 with Bi=0. When Bi increases, the flow pattern becomes one vortex only and it is more compact as shown in Fig. 15. The corresponding temperature profile is shown that it is almost symmetric vertically and warm fluid rises near the bottom while colder fluid located near the top wall as shown in Fig. 14. The corresponding temperature profiles are shown in Fig. 16, where warm fluid rises near the bottom and right walls and cold fluid descends along the top and left walls. The last one of them indicates that the left of cavity always colder than right and warm fluid rises near the right wall. In this case, the CEF fluid flow results show that the fluid exhibit different behaviour when We number is used with or without the Bi number when Ra number increases to 10^6 .We are unable to get stable solution for $We \geq 0.01$, therefore we indicate the this value of the We number as $We_{crit.}$.

We have observed one cell structure at $Ra = 10^6$ for a viscous fluid and one vortex only and it is more compact as shown in Figs. 17-19. Fluid flow results show that the fluid exhibit similar behaviour with or without the Bi number is used. The corresponding temperature profiles are given in Figs. 18-20, and the temperature throughout most of the cavity is uniform obtaining a value which average of the top and bottom walls. As We number is used there is no much difference between the CEF and viscous pseudoplastic fluids with or without Bi number is used. The corresponding streamline and temperature profiles are shown in Figs.21-23 and Figs. 22-24 respectively. The effect of the Nusselt number on the heat transfer are given in Fig. 26 for the CEF fluid and comparison with the viscous pseudoplastic fluid cases which is shown in Fig. 25. There is no relationship between them. We believe that experimental results are necessary to clear the this phenomena.

CONCLUSION

In this paper, we have attempted to determine the effect of the conduction of Biot boundary condition, Shear-thinning and elastic (the first normal stress difference) for shear-free thermal convection in a square cavity differentially heated and filled with fluids, have a influence in shaping the flow field and determining the heat transfer characteristics . The two-dimensional unsteady convective motion generated by buoyancy forces on the fluids. Investigation was made numerically by using a second order accurate scheme for viscoelastic namely CEF model when N_1 is in the form of eq.

(2.8) and finite difference method was used for the discretisation of time and space respectively. A range of Ra and We up to 10^6 and 0.001 has been investigated for both vertical walls maintained with Biot boundary conduction or not. Their combined effect (with Bi=0) acts to increase and decrease the heat transfer as represented by the local Nusselt number with the results that overall heat transfer for the viscous and CEF fluid cases are quite close at $Ra=10^6$. Also Biot boundary condition effect acts to increase the number of cells for the inelastic fluids case at $Ra=10^4$ and 10^5. Beyond the critical We number, we have observed that instability occurs in the flow and the system becomes unstable and loses its equilibrium. We believe that more works needs to be done in this subject such as pseudospectral finite difference (PSFD) in order to explain bifurcation phenomena which has been noted in (Siginer et.al., 1994).The work already under the consideration for the solid wall case as well as shear-free boundary condition.

REFERENCES

Shoney, A.V, 1988, Natural Convection Heat Transfer to Viscoelastic Fluid, *Encyclopedia of fluid Mechanics*, Ed. Cheremisinoff, N. P. ,Gulf, Houston.

Gebhard B.&Jaluria Y.&Mahajan R.L. &Sammakia B., 1988, Bouyancy-Induced Flows and Transport ,Hemisphere, Washington.

Demir H., Akyildiz F.T., Unsteady Thermal Convection Of A Non-Newtonian Fluid, *Int. J. of Engineering Science*, in printing.

Demir H., 1996, The Stability Properties of Some Rheological Flows, *Ph. D. Thesis*, , School of Accounting and Mathematics, Division of Math. And Computing, The University of Glamorgan, Wales/U.K.

Vahl Davis G. DE, 1983, Natural Convection of Air In a Square Cavity: A Bench Mark Numerical Solution, *Int. J. For Num. Meth. In Fluids*, 3, 249.

Torrance K. G.&Turcotte D. L. 1971, Thermal Convection with Large Viscosity Variations, *J. Fluid Mech.* 47(1), 113-125.

Mc Kensie D. P. et. all, 1974, Numerical Experiments on convection in the Earth's Mantle, *J. Fluid Mech.* 62, 465-538.

Bird R. B. & Steward W. E. & Lightfoot E. D , 1960 *Transport Phenomena* , John Wiley and Sons.

Rajagopalan D. & Amstrang R. C. & Brown R. A., 1990 *J. Non-Newtonian Fluid Mech*, 36, 159.

Douglas J. JR.&Peacemant D. W., 1966, Numerical Solution of Two Dimensional Heat Flow Problems *AIChE Journal*, 12, 161.

Charles L. Tucker III, 1989 , *Fundamentals of Computer Modelling For Polymer Processing*, Hanser Publishers, Munich-Vienna-New York.

Siginer D. A.& Valenzuaela-Rendon A., 1994, Natural Convection of Viscoelastic Fluid, *Numerical Methods for Non-Newtonian Fluid Dynamics*, FED-Vol.179,ASME.

Mortom K. Y., Mayers D. F.,1994, *Numerical Solution of Partial Differential Equations*, Cambridge University Press

Scraton R. E., 1987, *Further Numerical Methods in Basic*, Edward Arnold.

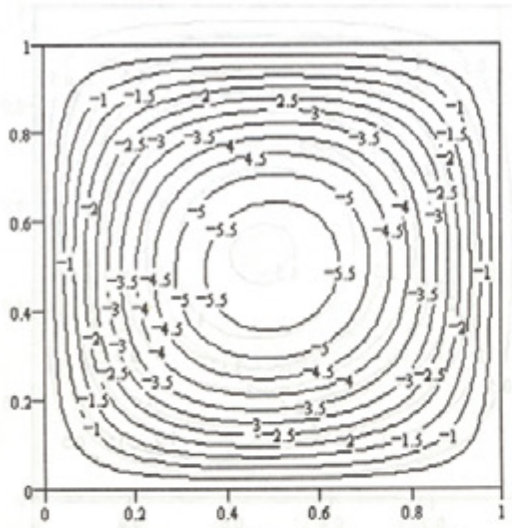

Figure 1; Streamline contours for viscous pseudoplastic fluid for We=0 Ra=10^4 Bi=0

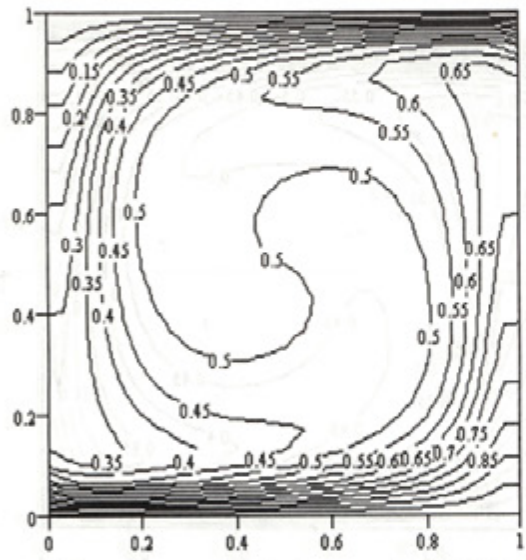

Figure 2; Temperature contours for viscous pseudoplastic fluid for We=0 Ra=10^4 Bi=0

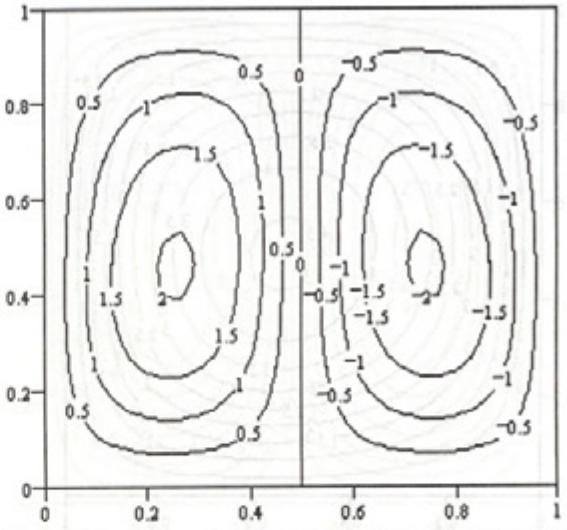

Figure 3; Streamline contours for viscous pseudoplastic fluid for We=0 Ra=10^4 Bi=10

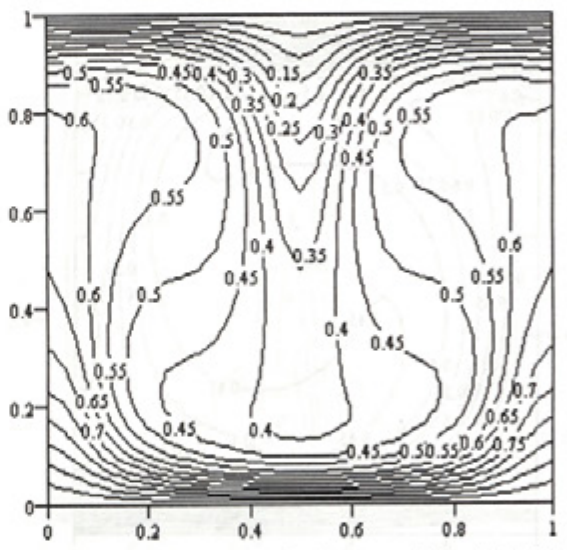

Figure 4; Temperature contours for viscous pseudoplastic fluid for We=0 Ra=10^4 Bi=10

Figure 5; Streamline contours for CEF pseudoplastic fluid for We=0.001 Ra=10^4 Bi=0

Figure 7; Streamline contours for CEF pseudoplastic fluid for We=0.001 Ra=10^4, Bi=10

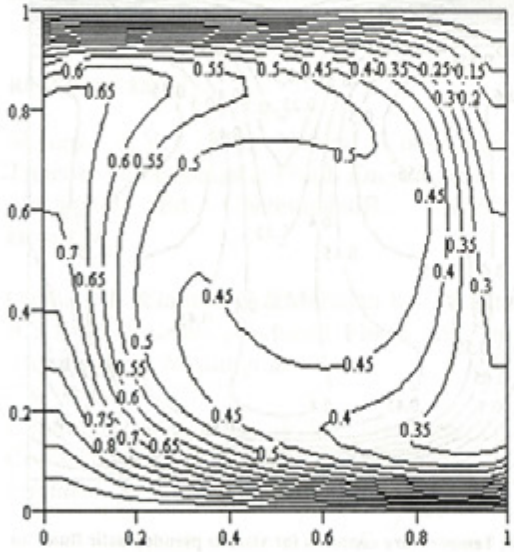

Figure 6; Temperature contours for CEF pseudoplastic fluid for We=0.001 Ra=10^4, Bi=0

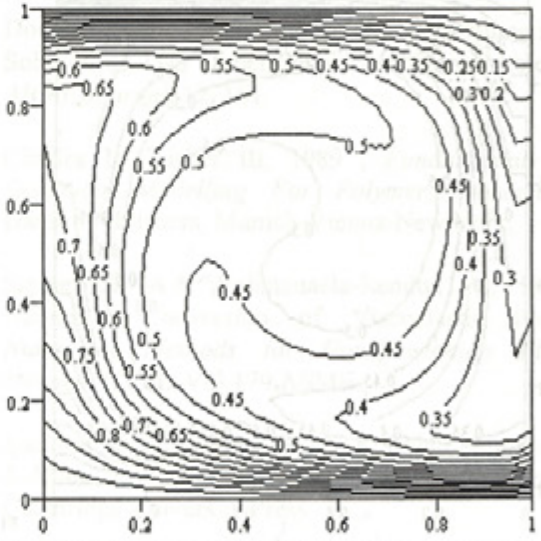

Figure 8; Temperature contours for CEF pseudoplastic fluid for We=0.001 Ra=10^4, Bi=10

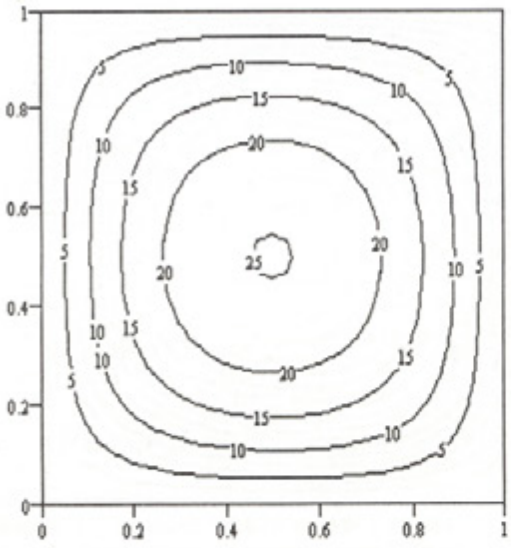

Figure 9; Streamline contours for viscous pseudoplastic fluid for We=0 Ra=10^5 Bi=0

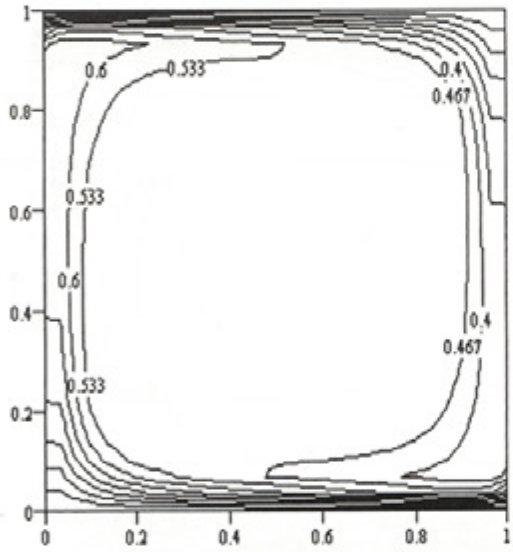

Figure 10; Temperature contours for viscous pseudoplastic fluid for We=0 Ra=10^5 Bi=0

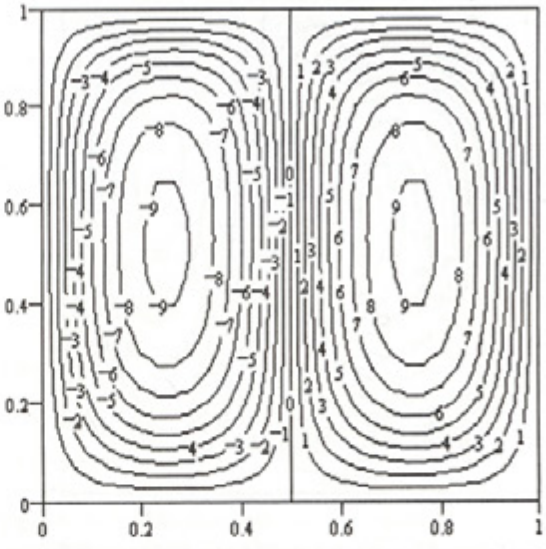

Figure 11; Streamline contours for viscous pseudoplastic fluid for We=0 Ra=10^5 Bi=10

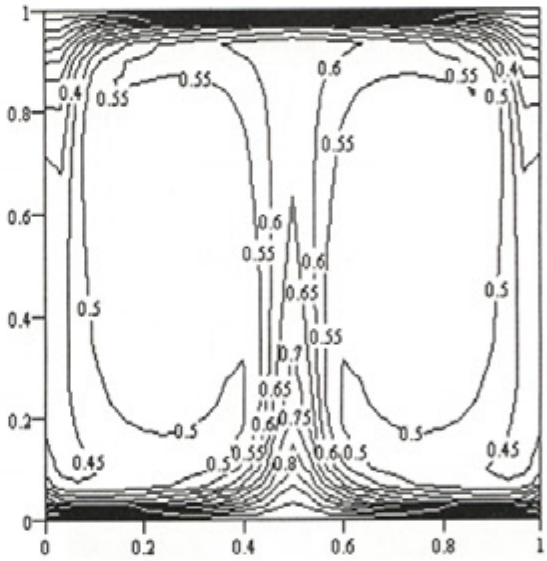

Figure 12; Temperature contours for viscous pseudoplastic fluid for We=0 Ra=10^5 Bi=10

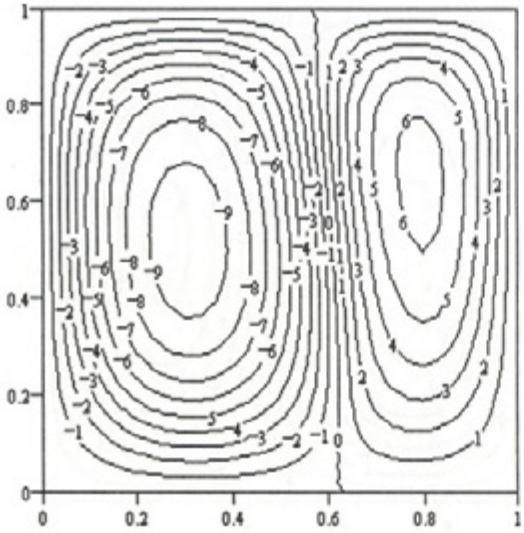

Figure 13; Streamline contours for CEF pseudoplastic fluid for We=0.001 Ra=10^5 Bi=0

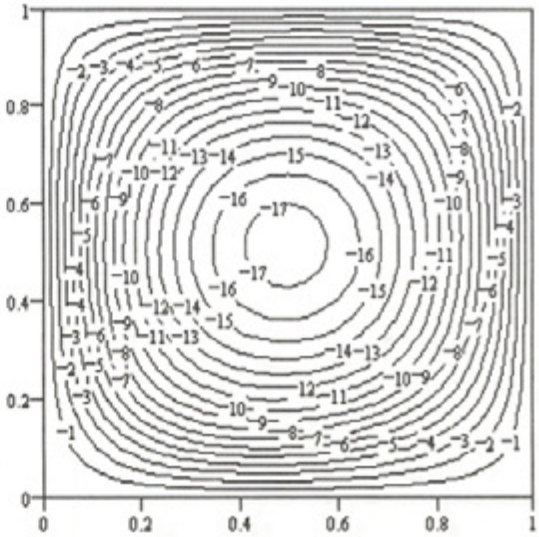

Figure 15; Streamline contours for CEF pseudoplastic fluid for We=0.001 Ra=10^5 Bi=10

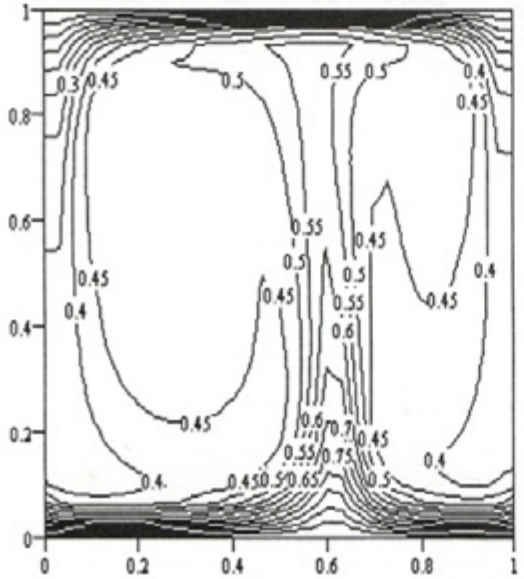

Figure 14; Temperature contours for CEF pseudoplastic fluid for We=0.001 Ra=10^5 Bi=0

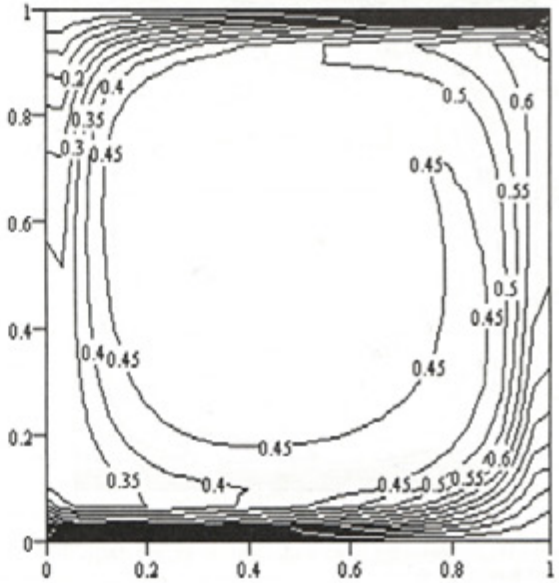

Figure 16; Temperature contours for CEF pseudoplastic fluid for We=0.001 Ra=10^5 Bi=10

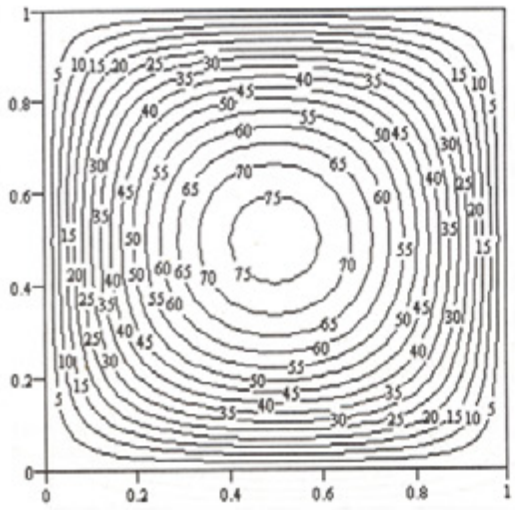

Figure 17; Streamline contours for viscous pseudoplastic fluid for We=0 Ra=10^6 , Bi=0

Figure 19; Streamline contours for viscous pseudoplastic fluid for We=0 Ra=10^6 , Bi=10

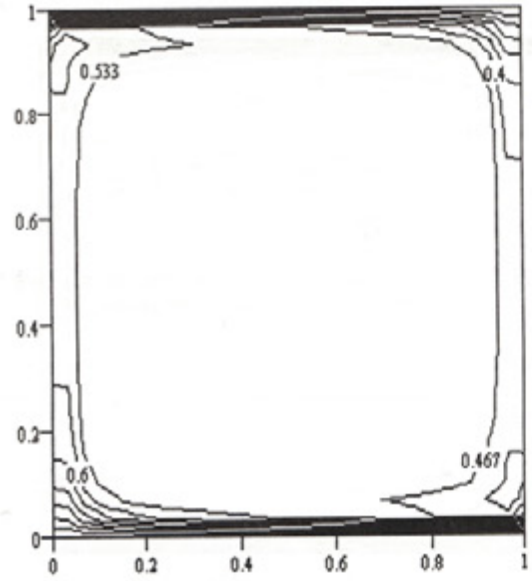

Figure 18; Temperature contours for viscous pseudoplastic fluid for We=0 Ra=10^6 ,Bi=0

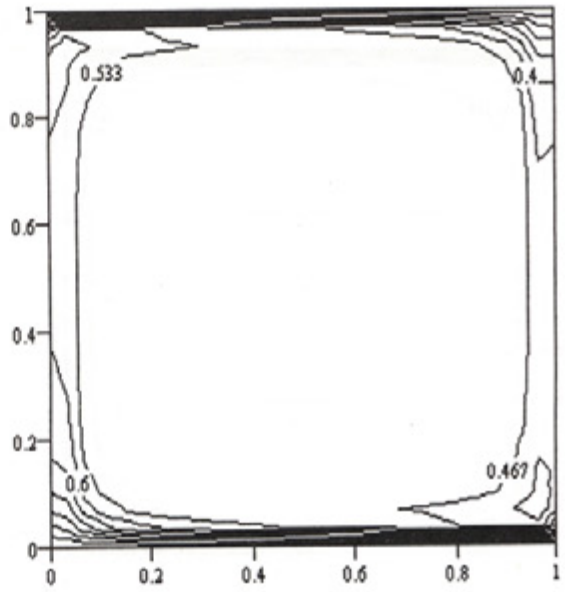

Figure 20; Temperature contours for viscous pseudoplastic fluid for We=0 Ra=10^6 ,Bi=10

Figure 21; Streamline contours for CEF pseudoplastic fluid for We=0.001 Ra=10^6 , Bi=0

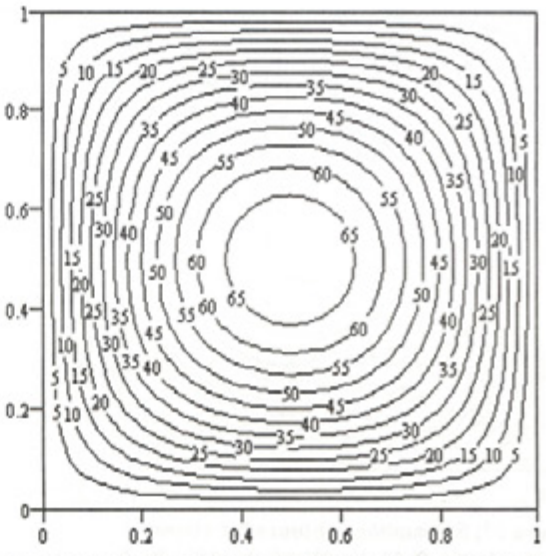

Figure 23; Streamline contours for CEF pseudoplastic fluid for We=0.001 Ra=10^6 , Bi=10

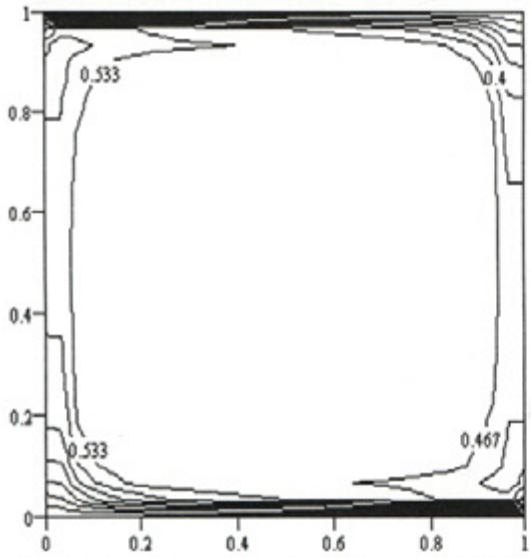

Figure 22; Temperature contours for CEF pseudoplastic fluid for We=0.001 Ra=10^6 ,Bi=0

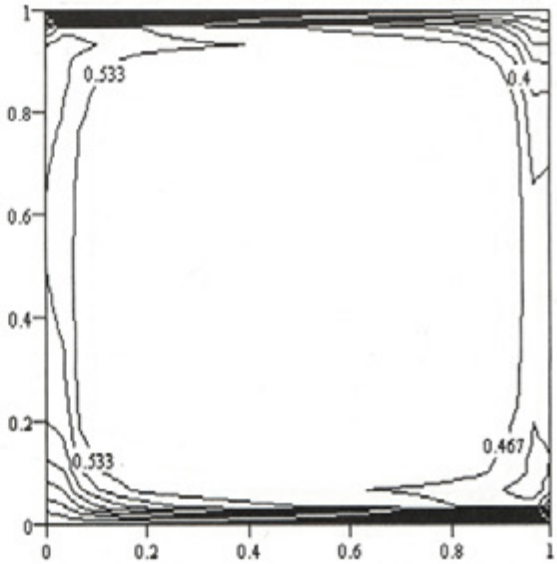

Figure 24; Temperature contours for CEF pseudoplastic fluid for We=0.001 Ra=10^6 ,Bi=10

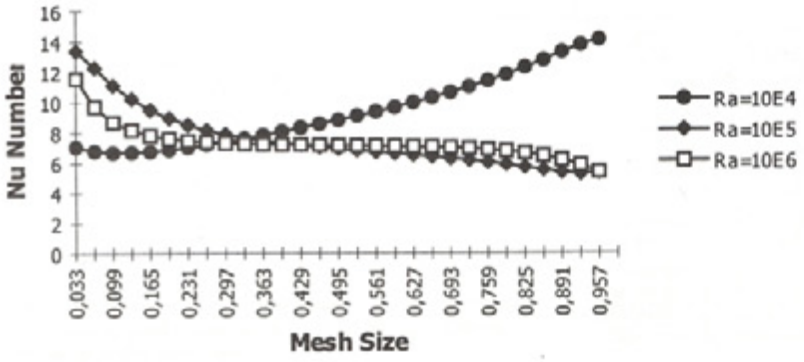

Figure 25; The effect of the Nusselt number on the heat transfer for viscous pseudoplastic fluid for We=0 Bi=0

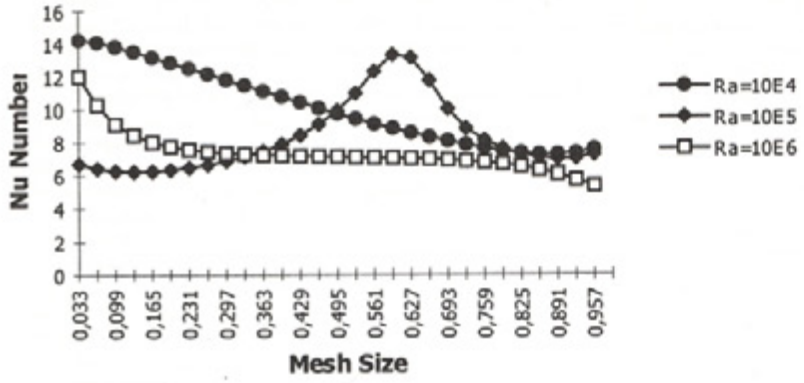

Figure 26; The effect of the Nusselt number on the heat transfer for CEF pseudoplastic fluid for We=0.001 Bi=0